DOI: 10.13009/EUCASS2019-462

Combustion Instability for Hybrid Rocket Motors with a Diaphragm

Jungpyo Lee[a,], Sunjae Rhee[b], Jinkon Kim[c], Heejang Moon[d],*
Olexiy Shynkarenko[e], Domenico Simone[f], Takakazu Morita[g]
[a,e,f]University of Brasilia, Brasilia, Federal District, 70910-900, Brazil
*[a,]*jpleerocket@gmail.com, [e]olexiy@aerospace.unb.br, [f]domenico.simone@aerospace.unb.br*
[b]Propulsion Center, Daejeon Plant, Hanwha Corporation, South Korea
[b]vsunjae@gmail.com
[c,d]School of Aerospace & Mechanical Engineering, Korea Aerospace University, South Korea
[c]jkkim@kau.ac.kr, [d]hjmoon@kau.ac.kr
[g]Department of Aeronautics and Astronautics, Tokai University, Hiratsuka, Japan
[g]morita@tsc.u-tokai.ac.jp

Abstract

A diaphragm has been used to enhance fuel regression rate and combustion efficiency in hybrid rockets. On the other hand, it has been observed that significant pressure oscillations occurred. In this paper, main factor on the excitation of the instability was studied. Lab-scale firing tests considering the various experimental conditions, such as the diaphragm location and diameter, were conducted, and combustion visualization tests were performed to confirm the instability mechanism. The excitation source of the pressure oscillations was the edge-tone instability. Finally, a new grain which had high regression rate and also was stable combustion was proposed.

Nomenclature

$D_{d.p}$	diaphragm port diameter	$\dot{m}_{ox}$	oxidizer mass flow rate
$D_{f.p}$	fuel port diameter	p_s	oxidizer supply pressure
$D_{N.T}$	nozzle throat diameter	Re	Reynolds number
$D_{f.diap}$	front diaphragm port diameter	t_b	burning time
$D_{r.diap}$	rear diaphragm port diameter	u_∞	free stream velocity
$G_{ox.avg}$	average oxidizer mass flux	ρ_∞	free stream density
L_f	fuel length	τ	period of impingement

1. Introduction

A hybrid propulsion system stores one propellant component in the liquid phase while stores the other in the solid phase. Because of this separation of oxidizer and fuel into two different states, combustion differs from that of either the solid or liquid rocket. This distinguishing characteristic gives rise to several advantages. The main advantages of these propulsion systems are safety, throttling, shutdown and restart, and low cost, while hybrid systems also have some disadvantages. Low regression rate is a representative disadvantage of hybrid systems. The limit on regression rate for the conventional hybrid combustion configuration is set by the physical phenomena of heat and mass transfer from the relatively remote flame zone to the fuel surface [1-3]. Various methods for increasing the fuel regression

DOI: 10.13009/EUCASS2019-462

rate have been suggested as follows; addition of energetic additives to solid fuel grain, liquefying fuels, introduction of swirl in the oxidizer flow, helical grain, or diaphragm in the fuel port [4].

A diaphragm can be used to increase the fuel regression rate and the combustion efficiency installing in the fuel port easily as shown in Fig. 1. Downstream diaphragm regression rate was increased due to strong and hot recirculation zone formed downstream of the diaphragm that entrains the hot gases from the reaction zone towards the fuel surface [5]. However, large pressure oscillations have been frequently observed in hybrid engines with a diaphragm, while the fuel regression rate was increased greatly [6]. The pressure time traces of firing tests for the hybrid motor with and without diaphragm are compared in Fig. 2. The pressure oscillation of the motor with a diaphragm is limit cycle behavior and large pressure fluctuations about 40 % of the mean chamber pressure. It is clear that the diaphragm has a strong influence on the instability since it couldn't find such a large oscillation in the same motor without diaphragm as Fig. 2. It is widely known that traditional hybrid rockets do not have violent pressure oscillations [7, 8].

In this research, the characteristic of the instability are studied considering various experimental conditions, and the instability mechanism for hybrid rocket motors with the diaphragm was analyzed. After the instability mechanism is investigated and understood, a new design which has high regression rate and can reduce the instability is suggested

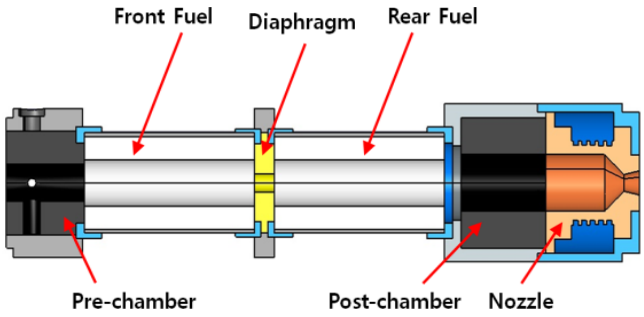

Figure 1: Configuration of hybrid rocket motor with diaphragm.

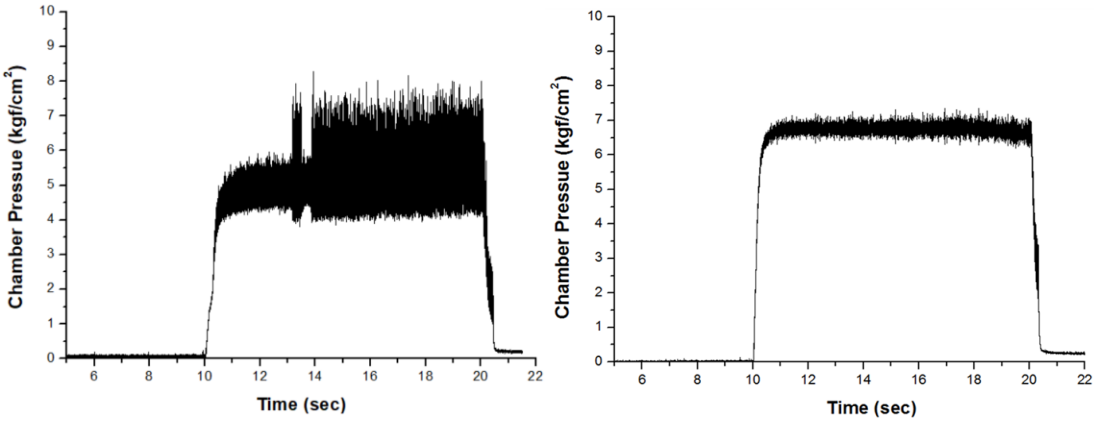

Figure 2: Chamber pressure time traces for motor with diaphragm(L) and without diaphragm(R).

2. Experimental conditions for the hybrid rocket motor instability

The test bench used in this research is mainly composed of the hybrid combustion chamber, the oxidizer feed system, the ignition system, and the data acquisition (DAQ) system. The combustion chamber is composed of the pre-combustion chamber, the fuel, the post-combustion chamber, and the nozzle, as in Fig. 3, and the axial type single-port injector was installed. A water-cooled copper alloy nozzle was used against erosion of the exhaust nozzle, and a carbon diaphragm which is the superior thermal durability was used. The chamber pressure oscillation was measured in both the pre-combustion chamber and post-combustion chamber using piezoelectric dynamic pressure transducers to capture pressure oscillations during test firings, the Kistler 6061B type. The analog signals coming from the sensors were sampled at frequency of 5 kHz, digitally converted (16 bit resolution), processed, and recorded by the NI PCIe-6320 data acquisition card system. The strain type pressure transducers were installed in the feeding pipe for

DOI: 10.13009/EUCASS2019-462

measuring the static pressure. The whole experimental process was automatically controlled by using program logic controllers where LabVIEW software was used [7].

Table 1 shows the specification of firing tests conducted. The gas oxygen (GOx) was chosen as oxidizer and the High Density Polyethylene (HDPE) as fuel. Proper function of the diaphragm in a hybrid rocket motor requires adjustment of its position, and the diaphragm is normally located in the midst of the grain to enhance the fuel regression rate. However, in this research, diaphragms were mounted at the front of the fuel or the rear to investigate mechanism of the instability observed in the hybrid motors with the diaphragm, and the four type motors were used as follows; type 1) a traditional hybrid rocket motor, that is, no diaphragm in the motor; Type 2) a diaphragm was mounted at the rear of the fuel; Type 3) a diaphragm was mounted at the front; Type 4) two diaphragms were mounted at both the front and rear. To investigate the characteristics of the instability, the various diaphragm diameters, the fuel port diameters, the fuel lengths, and the oxidizer mass flow rates were used, as in Table. 1.

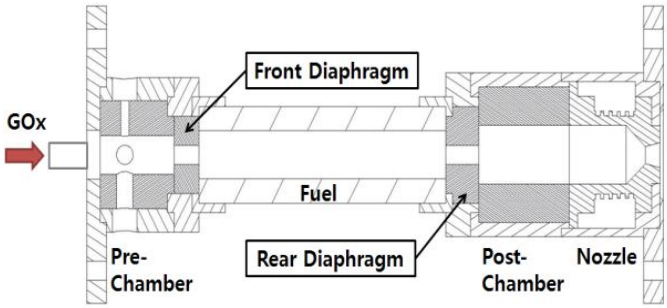

Figure 3: Schematic of hybrid rocket motor with diaphragms.

Table 1: Experimental conditions.

Oxidizer/Fuel	GOx/HDPE (Gas Oxygen/High Density Polyethylene)
$D_{f.p}$ (mm)	20, 25, 30
$D_{f.diap}/D_{r.diap}$ (mm)	10/10, 15/10, 7/10, 5/10, 10/15
$\dot{m}_{ox}$ (g/s)	5 ~ 65
L_f (mm)	300, 250, 200, 175, 150, 100, 75
t_b (s)	10
Sampling rate (/s)	5000

3. Experimental Result

3.1 Characteristic Differences of the Combustion Instability according to the Diaphragm Position

There are used the four type motors to investigate mechanism of the instability, as mentioned above. Fig. 4-7 show the pressure time traces and the Fourier transform result of the pressure signal for each of the type motor. All other test conditions except the diaphragm location are the same; L_f =200 mm, $D_{f.p}$=25mm, $D_{N.T}$=9 mm, $\dot{m}_{ox}$ =26 g/s, P_s=30 bar, $D_{f.diap}$=10 mm, $D_{r.diap}$=10 mm.

Type 1 is a traditional hybrid rocket motor. The oscillation frequencies frequently observed in a traditional hybrid rockets are as follows [8]; the TC coupled instability, the Helmholtz mode, the longitudinal acoustic mode, and the feed system coupled instability. The mechanism of the TC coupled oscillation is based on the coupling of the thermal lag by the heat capacity of the solid fuel and the transients in the gas-phase combustion in boundary-layer. The Helmholtz mode is occurred as flow comes in large volume through narrow neck and the waves in the volume are repeated compression and expansion, and the longitudinal acoustic mode is caused by acoustic waves that travel with the axial direction in combustor. And the feed system coupled instability is a dynamic instability of the coupled flow system-combustion in which the time-dependent response of the propellant is related to the changing combustor pressure, and it is commonly observed in the liquid feed rockets. In the Fourier transform result of Type 1, the

DOI: 10.13009/EUCASS2019-462

oscillation around 100 Hz was estimated as the TC coupled instability using a TC coupled model developed newly in this study, and the oscillation around 1000 Hz was the first longitudinal acoustic mode. The new TC coupled model is described later on. The feed system coupled instability couldn't be found since the gas oxygen was used and the feed system can reliably be isolated from the motor by the insertion of a sonic orifice.

Type 2 and Type 4 mounted the diaphragm at the rear of the grain resulted in the violent chamber pressure oscillations with peak to peak values as high as 5 bar to about 83% of the mean pressure and 4 bar to about 67 %, respectively, as shown in Fig. 5 and Fig. 7, whereas Type 1 and Type 3 not installed in the rear didn't show such a strong pressure oscillation. It can be confirmed that Type 2 and 4 have an excitation source frequency of 83 Hz and of 176 Hz from the Fourier Transform results, respectively, and the resonance could be observed at the frequency for each type. It can be seen that the rear diaphragm has a strong influence the instability, and the flow collision on the rear diaphragm surface may have an important factor to induce the large pressure oscillations.

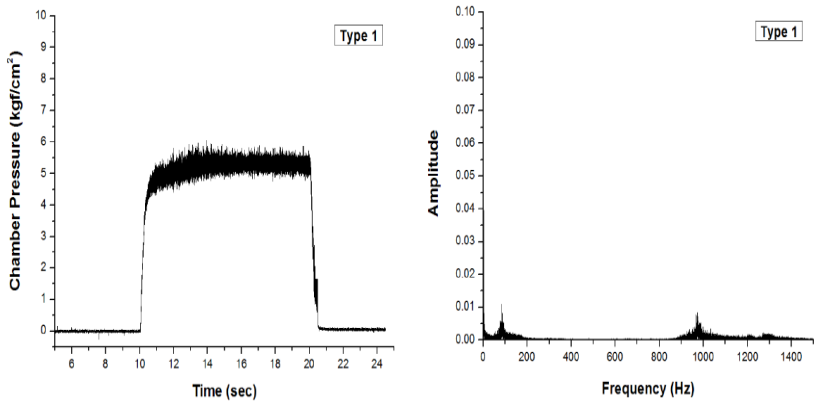

Figure 4: Chamber pressure time traces(L) and FFT analysis(R) for Type 1.

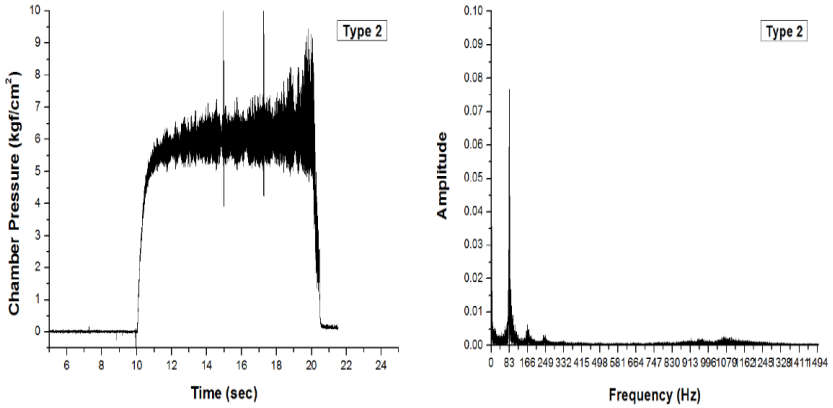

Figure 5: Chamber pressure time traces(L) and FFT analysis(R) for Type 2.

DOI: 10.13009/EUCASS2019-462

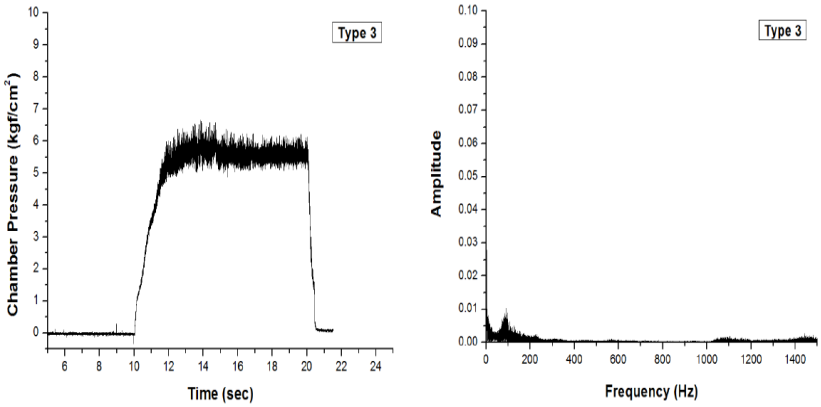

Figure 6: Chamber pressure time traces(L) and FFT analysis(R) for Type 3.

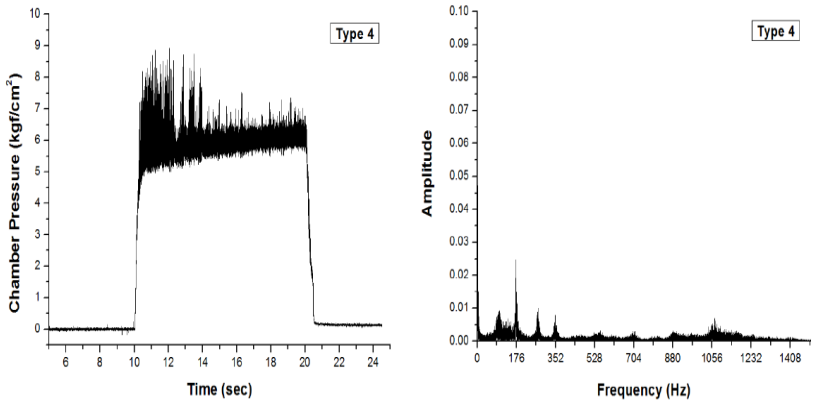

Figure 7: Chamber pressure time traces(L) and FFT analysis(R) for Type 4.

3.2 Effects of the Rear Diaphragm's Diameter Variation on the Instability

The propellant flow in motors with a rigid obstacle at the rear, such as the diaphragm, could collide with it, and it induces pressure fluctuation. To verify the hypothesis, experimental tests were conducted with different rear diaphragm's diameters. Most of the test parameters, such as $D_{f.p}$, L_f, $\dot{m}_{ox}$, $D_{N.T}$, and P_s, were analogous except the rear diaphragm diameter. The front diaphragm diameter was fixed as 10 mm, and the two different rear diaphragm diameters of 10 and 15 mm were used. Fig. 8 and Fig. 9 show the pressure time traces of the tests and the Fourier Transform results, respectively. It can be seen that there's not much difference in the resonance frequencies, however, the pressure oscillation amplitude is larger when the rear diaphragm diameter is smaller. It is considered that the rear diaphragm diameter has a strong influence in the oscillation amplitude, not in the frequency, since strength of the collision of the propellant flow with the rear diaphragm increases as the diameter is small, that is, as the collision area increases.

DOI: 10.13009/EUCASS2019-462

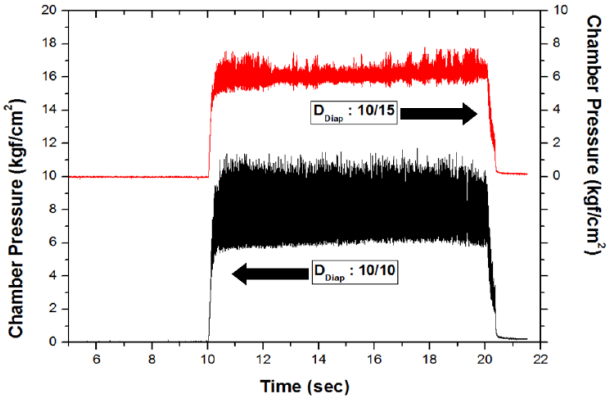

Figure 8: Chamber pressure time traces on variation of $D_{r.diap}$.

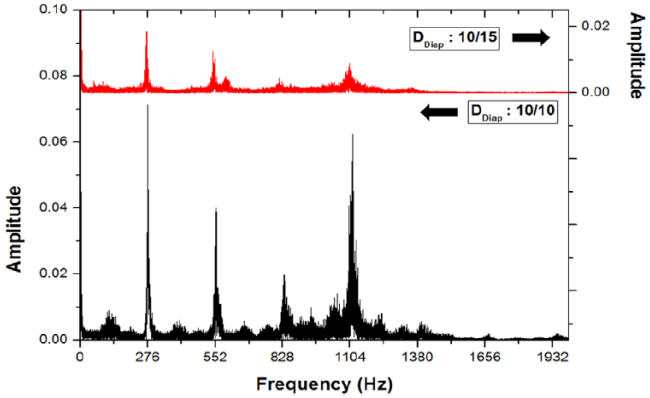

Figure 9: FFT analysis of chamber pressure.

3.3 Effects of the Front Diaphragm's Diameter Variation on the Instability

It could be confirmed from the previous section 3.1 that the motors which are installed only the front diaphragm couldn't induce the instability with large pressure oscillations. However, the diameter of the front diaphragm is expected to have an impact on the frequency or amplitude of the instability in motors with a rear diaphragm. In this section, effects of variation of the front diaphragm diameter on the instability are investigated. Fig. 10-13 show the chamber pressure time traces for the four test conditions; case (1) $D_{f.diap}/D_{r.diap}$=5/10 mm; case (2) $D_{f.diap}/D_{r.diap}$=7/10; case (3) $D_{f.diap}/D_{r.diap}$=10/10; case (4) $D_{f.diap}/D_{r.diap}$=15/10. The diameter of the rear diaphragm for all cases is the same as 10 mm, and all other test conditions except the front diaphragm diameter are the same; L_f=175 mm, $D_{f.p}$=25mm, $D_{N.T}$=9 mm, $\dot{m}_{ox}$ =0.26 kg/s, P_s=30 bar. There are large pressure oscillations in Case #2, Case #3, and Case #4 since the flow through the fuel port collides with rear diaphragms. However, Fig. 10 shows that Case #1 with the smallest front diaphragm diameter as 5 mm is very stable, which oscillates less 2% of the mean chamber pressure. It can be said that it couldn't implement the mechanism to induce the instability if the flow injected through the front diaphragm is faster than a critical velocity. And also it is possible to conclude that the front diaphragm diameter has an important role on the fundamental frequencies of the oscillations since the frequency decreases as the front diaphragm diameter increases, as shown in the figures. The explanation for these results will be described next section.

DOI: 10.13009/EUCASS2019-462

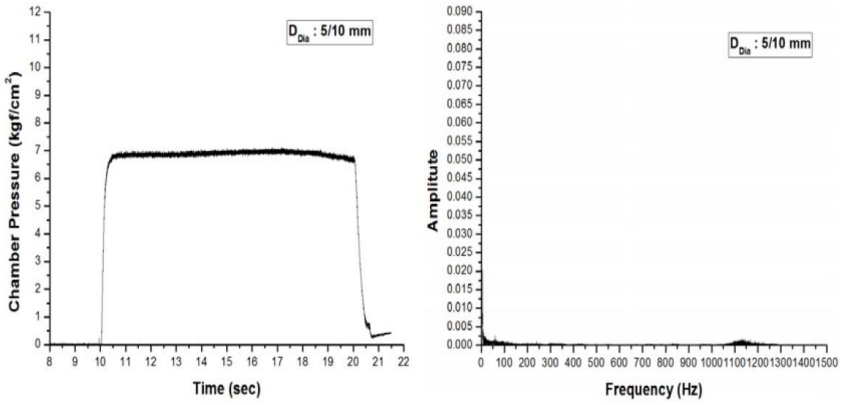

Figure 10: Chamber pressure vs. time(L), FFT analysis(R), $D_{f.diap}/D_{r.diap}$: 5/10 mm.

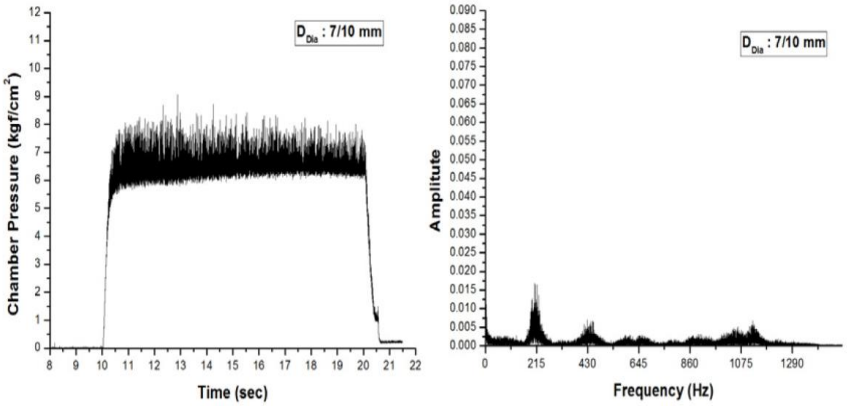

Figure 11: Chamber pressure vs. time(L), FFT analysis(R), $D_{f.diap}/D_{r.diap}$: 7/10 mm.

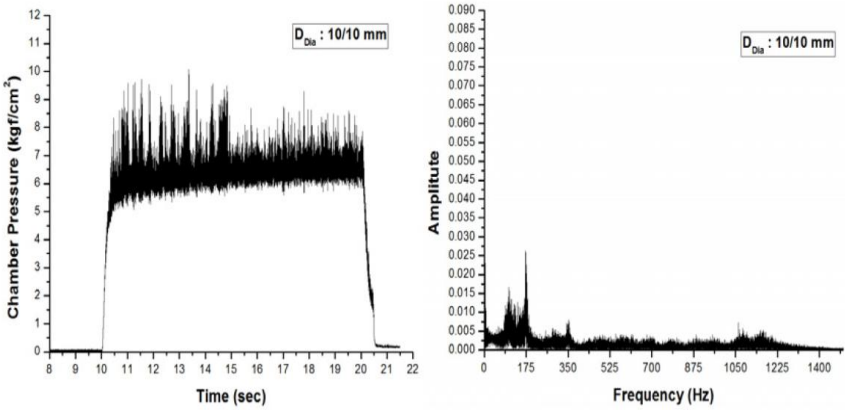

Figure 12: Chamber pressure vs. time(L), FFT analysis(R), $D_{f.diap}/D_{r.diap}$: 10/10 mm.

DOI: 10.13009/EUCASS2019-462

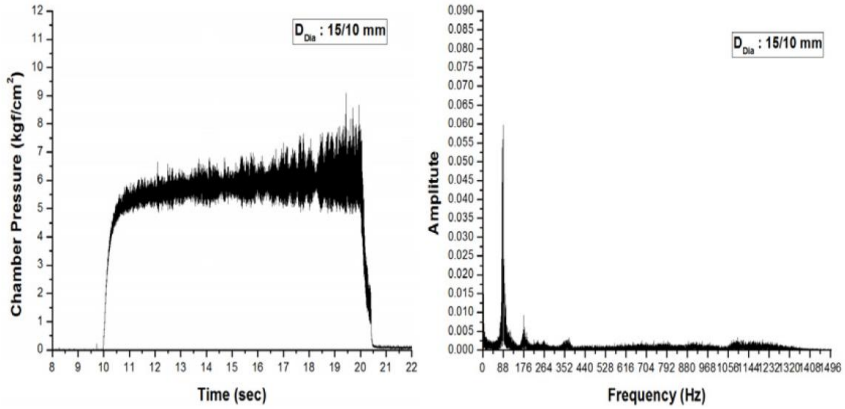

Figure 13: Chamber pressure vs. time(L), FFT analysis(R), $D_{f.diap}/D_{r.diap}$: 15/10 mm.

3.4 The mechanism of the instability for the motor with the diaphragm

From the experiments above, it can be inferred that the propellant flow impinging to the rigid rear diaphragm is an important role to excite the pressure oscillation in the motor with the diaphragm. The unstable jets of free shear layers at the front diaphragm edge, such as vortices, are generated. The vortices impinging on the rear rigid diaphragm surface generate the variation of pressure, and drive discrete oscillation by the feedback mechanism between the unstable jet and the acoustic wave. This phenomenon is named the edge-tone, and it has been widely studied since it can produce a strong vibration in various flow fields [9-15].

As shown in Section 3.3, the motor with the front diaphragm diameter as 5 mm has very stable combustion even though there is the rear diaphragm. It can be explained regarding the edge-tone instability. The flow injected through the front diaphragm of the small port diameter has a large axial velocity and momentum relatively. And therefore, the disturbance on the flow is not enough to generate vortices to oscillate the pressure. The jet formed through the small diameter of the front diaphragm could be passed without any noticeable impingements on the rear diaphragm surface.

The mechanism of the combustion instability induced in the hybrid motor where the diaphragm is located in the midst of the grain can be explained as shown in Fig. 14. The vortices are created at a single axial injector exit with an abrupt step, and the periodical impingement of the vortices to the rigid diaphragm drives the pressure oscillation. And this oscillation amplitude could be highest when an edge-tone frequency happens to resonate with a natural frequency in the hybrid combustion system.

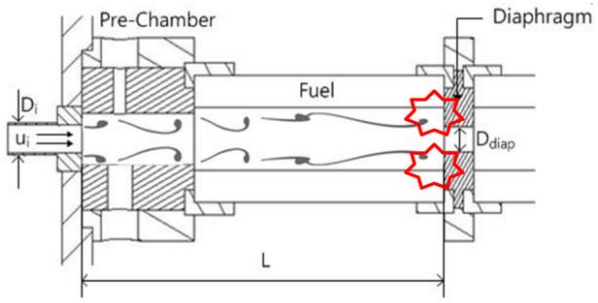

Figure 14: Mechanism of Instabilty for Motors with Diaphram.

4. Visualization Test for a Motor with the Diaphragm

Combustion visualization tests for a motor with diaphragm were conducted to verify the hypothesis of the instability of the edge-tone. Fig. 15 shows the configuration of the visualization test motor. A front diaphragm and a rear were mounted on the fuel surface, and the fuel grain configuration was designed as a simple flat plate to take from the side

DOI: 10.13009/EUCASS2019-462

of motor. The High Density Polyethylene (HDPE) was chosen as a fuel and the gas oxygen (GO_x) as an oxidizer, and the oxidizer mass flow rate was about 20 g/sec ($G_{ox.avg}$=10 kg/m^2-sec). The ratio of the diaphragm port area to the fuel port area was 4 to satisfy dynamical similarity for the lab-scale motor, and the thickness of the diaphragm was 10 mm. The window of SiO_2 material which works at a high temperature 1200 K was used, and the window dimension was 259×109×19 mm. The visualization test was filmed at 6000 sampling rate using a high speed camera, FASTCAM APX-RS model, Photron [16].

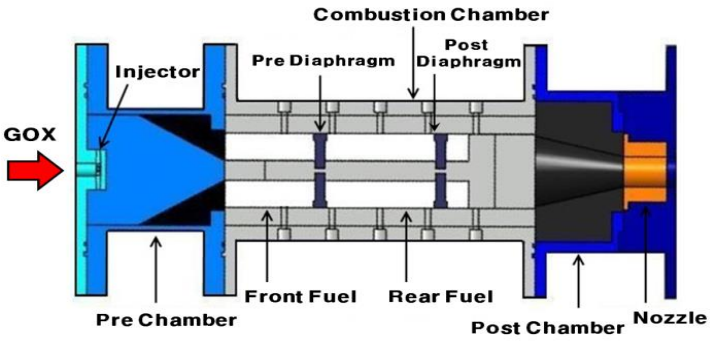

Figure 15: Test Motor for Combustion Visualization.

Fig. 16 shows the images of the combustion visualization test in chronological order; in (a), a vortex is created at the edge of the front diaphragm; in (b) and (c), the vortex detached from the diaphragm is moving toward the rear diaphragm; in (d), the vortex passed collides with the rear diaphragm. This collision can induce a distinct pressure oscillation. After a vortex is collided, acoustic wave is generated at the surface of the rear diaphragm. The generated acoustic wave propagates forward and excites the shear layer at the edge of the front diaphragm, and it can induce a new vortex. The feedback loop between the flow and the acoustic wave leads to self-sustained pressure oscillations of large amplitudes, therefore, it can continue to supply energy to maintain the periodic pressure oscillation [15].

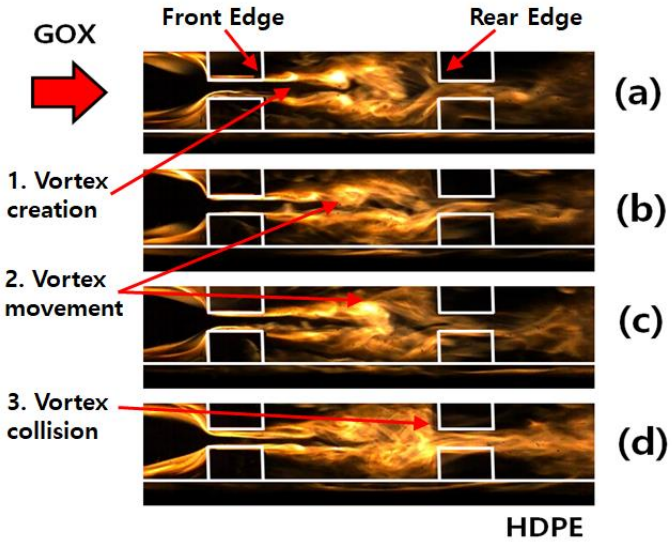

Figure 16: Images of Combustion Visualization Test.

5. Resonance of the Edge-tone with the natural instability of hybrid rockets

The resonances were observed in the most experiments for the motors using the rear diaphragm. As the frequency of the excitation source, the edge-tone, is equal or nearly equal to one of the natural frequencies of the hybrid rocket system, the resonance can be occurred with the violent pressure oscillation. The natural frequencies of the system are considered as follows; the TC coupled instability, the Helmholtz mode, and the longitudinal acoustic mode. It was investigated that the excitation source was the impingement of vortices from Ref. [17] before. In this study, it is

DOI: 10.13009/EUCASS2019-462

newly investigated which natural frequency occurs the resonance, and a new TC coupled frequency model is developed. The TC coupled instability theory in hybrid rocket motors was developed by Karabeyoglu, and the TC coupled frequency model was proposed in Ref. [18]. It shows the inverse relationship between the frequency and the boundary layer delay time, as shown in Eq. (1). It can be confirmed that the boundary layer response time (τ_{bl}) is an important factor to predict the frequency, and it is composed of the surface friction velocity (u_τ) and the boundary layer thickness (δ). However, the τ_{bl} model in Ref. [18] can be applied to the limited cases of an incompressible turbulent boundary layer with no blowing. However, blowing effect should be considered for accurate model because the blowing on fuel surface has a strongly important role on the hybrid combustion.

$$f_{TC.w.blowing} = \frac{0.48}{\tau_{bl}} = \frac{0.48}{\delta/u_\tau} \tag{1}$$

$$\tau_{bl} = 2.18Re^{-0.1}\left(\frac{L_f}{2\sqrt{u_\infty}}\right)$$

The new TC coupled model considering the fuel blowing is expressed as Eq. (2). The Stevenson's law which is a model for injection/suction flow on the porous wall was applied to analyze the turbulent boundary with the blowing on the fuel surface [19]. And, in the development of τ_{bl} with blowing, the Simple Film Theory by LEES was used to calculate the ratio of the skin-friction coefficient with blowing (C_f) and without blowing (C_{f_0}), which is expressed using the blowing parameter (mass-transfer number, B) [20]. v_w is the vertical velocity of the flow ejected on the surface, and ρ_w is the density of the flow ejected. The coefficient c' in Eq. (2) can be determined empirically and is affected by parameters such as u_τ and v_w. It is more complex by comparison with the TC coupled model without blowing, Eq. (1), however, it can consider fuel blowing on surface with the parameters of v_w and b.

$$\tau_{bl} = \frac{\delta}{u_\tau} = c'\left(\frac{e^b - 1}{b}\right)Re^{-0.8}\frac{L_f}{2u_\infty}e^{0.88\left(\sqrt{\frac{u_\infty}{v_w}} - \frac{u_\tau}{v_w}\right)} \tag{2}$$

$$b = \frac{\rho_w v_w}{\rho_\infty u_\infty}\frac{1}{C_{f_0}/2}$$

The frequency of the edge-tone instability can be calculated using Eq. (3), which is modified from the Rossiter's model to meet this study [21]. Rossiter had researched the self-sustained oscillation generated in rectangular cavities, and the phenomenon is very similar to the edge-tone instability. u_i is the discharge velocity at the front diaphragm, and K is the ratio of the average speed of vortices in the chamber to the discharge velocity at the front diaphragm. L_f is the distance between the two diaphragms, that is to say the fuel length. c is the sound speed, and M is the Mach number. The period of impingement, τ, is a time interval between two successive collisions at the rear diaphragm. An acoustic wave by a vortex collision at the rear diaphragm propagates forward and excites the shear layer at the edge of the front diaphragm in the time t_1 (L_f/c), and a new vortex generated at the front diaphragm edge moves and collides to the rear diaphragm in the time t_2 (L_f/u_i K). Therefore, τ is the sum of t_1 and t_2. n is the number of vortices between the two diaphragms, and the frequencies at which the peaks occur lie in a sequence of the form n where n is an integer, and the value n of 1 was used in this study. The flow in the chamber was considered an ideal gas to calculate the average speed of the vortex, u_iK.

The fundamental frequencies in Fig. 11, Fig, 12, and Fig. 13 were 215, 175, and 88 Hz respectively. Using Eq. (3), it can explain the reason why the frequency decreases as the front diaphragm diameter increases. The frequency of the edge-tone is proportional to the discharge velocity at the front diaphragm, and the discharge velocity decreases as the diaphragm diameter increases.

$$f_{edge-tone} = \frac{n}{\tau} = \frac{n}{t_1 + t_2} = \frac{n}{\frac{L_f}{c} + \frac{L_f}{u_i K}} = \frac{u_i}{L_f}\frac{n}{\left(\frac{1}{K} + M\right)} \tag{3}$$

Fig. 17 shows that the frequencies predicted by the new TC coupled model are consistent with those by the edge-tone model, and the two models can predict the experimental fundamental pressure oscillation frequencies quite well, even though they were conducted with various and wide range of the test conditions, such as the variation of fuel port diameter, the diaphragm diameter, the oxidizer mass flow rate, and the fuel length, as shown in Table. 1. It needs to be noticed that tests for the motor having the rear diaphragm were plotted in Fig. 17, therefore data with large

DOI: 10.13009/EUCASS2019-462

oscillation were only considered. It can be concluded that the excitation source in the motors to induce the large pressure oscillations is the collision of vortices with the diaphragm, and the resonances occurred in most tests because the edge-tone frequency is near the TC coupled frequency which is a natural frequency in hybrid propulsion system. The frequency of the edge-tone is inversely proportional to the distance between the two diaphragms, and increases as the discharge velocity at the front diaphragm increases. And the TC coupled model of Eq. (2) has the same characteristics.

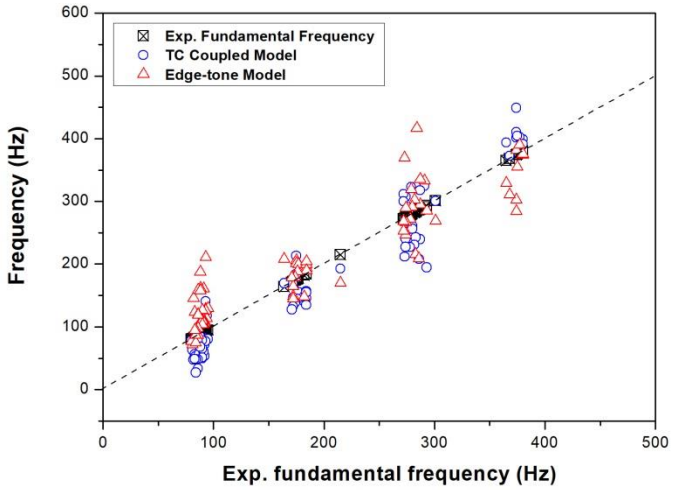

Figure 17: Comparison of fundamental frequencies and predicted frequencies.

6. New Stable Motor Design

A new motor design which is high regression rate and also eliminates the excitation source of the edge-tone instability was proposed, which is named ‘Stepped Grain’ in Fig. 18. The fuel is divided in two, and the rear fuel has larger diameter than the front fuel. Therefore, there is the same effect to increase the regression rate in hybrid motor with a diaphragm. A detailed description for the test of Stepped Grain can be found in Ref [22].

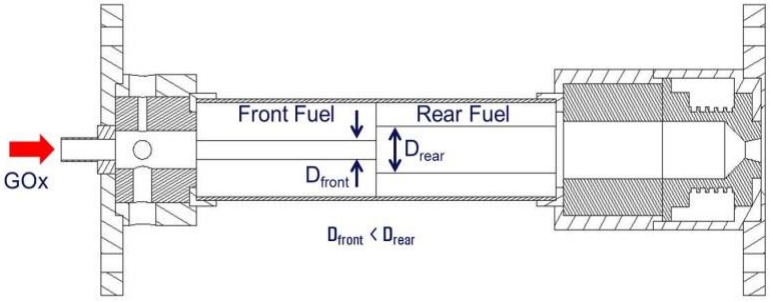

Figure 18: Stepped Grain Configuration.

Figure 19 shows the chamber pressure-time traces and the Fourier transform of the chamber pressure signal for a Stepped Grain test data. The front and the rear fuel diameter are 10 and 25 mm respectively. The chamber pressure was well damped, around 4% of the mean chamber pressure since there is no collision of vortex to rear obstacle, and the regression rate of the rear fuel was increased greatly compared to the traditional single port grain to 50 % [22]. It couldn’t find a frequency with high amplitude as shown in the Fourier Transform result.

DOI: 10.13009/EUCASS2019-462

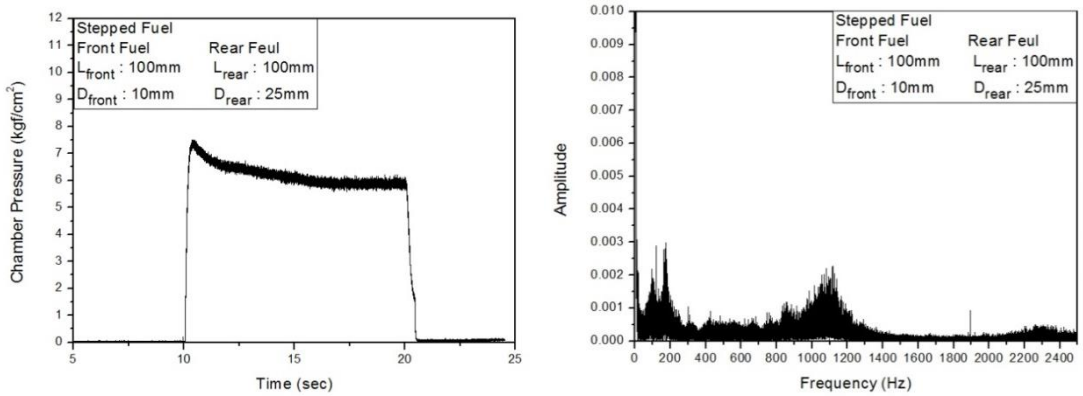

Figure 19: Chamber pressure and Fourier Transform analysis for Stepped Grain.

7. Conclusion

The large pressure oscillation with the resonance were observed in the hybrid motor installed a diaphragm, and the main factor on the excitation of the combustion instability was experimentally analysed. From the experimental results, it could be concluded that the excitation source of the oscillation in the motor was the periodical impingement of the vortices to the rigid rear diaphragm, which is named the edge-tone instability. The instability describes that the vortices itself couldn't drive a large pressure oscillation, and the periodical impingement of the vortices on the hard surface is necessary to induce it.

The resonances with the violent pressure oscillations occurred in most tests using the rear diaphragm because the edge-tone frequency is near a hybrid combustion system's natural frequency. The new TC coupled frequency model considering the blowing on the fuel surface was developed. It was confirmed that the fundamental frequencies of the tests coincided well with the frequencies calculated using the new TC coupled model and the edge-tone model. Therefore, it can be concluded that the large pressure oscillation in the hybrid motor with the diaphragm was occurred due to the resonance with the TC coupled frequency as the natural frequency of hybrid motor system and the edge-tone frequency as the excitation frequency.

The new grain design which is named 'Stepped Grain' was proposed to eliminate the edge-tone instability, which is to remove the rigid obstacle where the vortices impinge, in addition, it could increase fuel regression rate. The regression rate was increased greatly compared to the traditional single port grain, and it was very stable combustion.

References

[1] Ronald Humble, Gregory Henry, and Wiley Larson. 1995. Space Propulsion Analysis and Design. McGraw-Hill, Inc. Ch. 7.
[2] George P. Sutton and Oscar Biblarz. 2000. Rocket Propulsion Elements. Seventh Ed. John Wiley & Sons Inc.
[3] Marxman, G. A., Wooldridge, C. E., and Muzzy, R. J. 1964. Fundamentals of Hybrid Boundary Combustion. Progress in Astronautics and Aeronautics. Vol. 15. 485–522.S
[4] Claude Oiknine. 2006. New perspectives for hybrid propulsion. AIAA 2006-4674. In: 42nd AIAA/ASME/SAE/ASEE Joint Propulsion Conference & Exhibit.
[5] Matthias Grosse and Gerhard Schlatzke. 2008. Development of a Hybrid Rocket Motor Using a Diaphragm for a Small Test Rocket. AIAA 2008-4831. In: 44th AIAA/ASME/SAE/ASEE Joint Propulsion Conference & Exhibit.
[6] Moon, Keunhwan. 2012. A Study on Combustion Characteristic of the Hybrid Combustor Using Non-combustible Diaphragm. Master Dissertation. Korea Aerospace University.
[7] Jungpyo Lee. 2013. A Study on the Combustion Instability Attenuation of the Hybrid Rocket Using Diaphragm. Ph. D. Dissertation. Korea Aerospace University.
[8] M. Arif Karabeyoglu. 2007. Fundamental of Hybrid Rocket Combustion and Propulsion. Chap. 9. AIAA, INC.
[9] Michalke, A. and Fuchs, H.V. 1975. On Turbulence and Noise of an Axisymmetric Shear Flow. Journal of Fluid Mechanics. Vol. 70. Issue 01. 179-205.

DOI: 10.13009/EUCASS2019-462

[10] Crighton, D.G. 1975. Basic Principles of Aerodynamic Sound Generation. Progress in Aerospace Sciences. Vol. 16. 31-96.
[11] Rockwell, D. and Naudascher, E. 1979. Self-sustained Oscillations of Impinging Free Shear Layer. Annual Review of Fluid Mechanics. Vol. 11. 67-94.
[12] Rockwell, D. 1983. Oscillations of Impinging Shear Layer. AIAA Journal, Vol. 21. Issue 05. 645-661.
[13] Lush, P.A. 1971. Measurements of Subsonic Jet Noise and Comparison with Theory. Journal of Fluid Mechanics. Vol. 46. Issue 03. 477-500.
[14] Mani, R. 1976. The Influence of Jet Flow on Jet Noise. Part 1. The Noise of Unheated Jets. Journal of Fluid Mechanics. Vol. 73. Issue 04. 753-778.
[15] Im, Jung-Bin. 1999. A Study on Tone Generation and Flow Instability of Impinging Circular Jet. Ph. D. Dissertation. Soongsil University.
[16] Oh, Jisung. 2012. A Study on the Flow Visualization in Combustor of Hybrid Rocket with Diaphragm. Master Dissertation. Korea Aerospace University.
[17] Jungpyo Lee, Youngnam Kim, Jinkon Kim, and Heejang Moon. 2013. A Study on Combustion Instability of the Hybrid Rocket Motor with a Diaphragm. Journal of the Korean Society of Propulsion Engineers. Vol. 17. No. 6.
[18] M. Arif Karabeyoglu, Shane De Zilwa, Brian Cantwell, and Greg Zilliac. 2005. Modeling of Hybrid Rocket Low Frequency Instabilities. Journal of Propulsion and Power. Vol. 21. No. 6.
[19] Stevenson, T. N. 1963. A Law of the Wall for Turbulent Boundary Layer with Suction or Injection. Cranfield Coll. Aero. Rep. 166.
[20] Lees, L. 1958. Convective heat transfer with Mass Addition and Chemical Reactions. Combustion and Propulsion. Third AGARD Colloquim. Pergamon Press. New York, Elmsford.
[21] J.E. Rossiter. 1964. Wind-Tunnel Experiments on the Flow over Rectangular Cavities at Subsonic and Transonic Speeds. Reports and Memoranda. No. 3438.
[22] Jungpyo Lee, Sunjae Rhee, Jinkon Kim, and Heejang Moon. 2014. An Analysis and Reduction Design of Combustion Instability Generated in Hybrid Rocket Motor. Journal of the Korean Society of Propulsion Engineers. Vol. 18. No. 4. pp. 18-25.